European Journal of Radiology xxx (2015) xxx–xxx

Contents lists available at ScienceDirect

European Journal of Radiology

journal homepage: www.elsevier.com/locate/ejrad

Pancreatic neuroendocrine tumors containing areas of iso- or hypoattenuation in dynamic contrast-enhanced computed tomography: Spectrum of imaging findings and pathological grading

Ryota Hyodo*, Kojiro Suzuki, Hiroshi Ogawa, Tomohiro Komada, Shinji Naganawa

Department of Radiology, Nagoya University Graduate School of Medicine, 65 Tsurumai-cho, Showa-ku, Nagoya, Aichi 466-8550, Japan

ARTICLE INFO

Article history:
Received 15 June 2015
Accepted 19 August 2015

Keywords:
Pancreas
Neuroendocrine tumor
Dynamic contrast-enhanced CT
Pathological grading

ABSTRACT

Purpose: To evaluate dynamic contrast-enhanced computed tomography (CT) features of pancreatic neuroendocrine tumors (PNETs) containing areas of iso- or hypoattenuation and the relationship with pathological grading.

Materials and Methods: Between June 2006 and March 2014, 61 PNETs in 58 consecutive patients (29 male, 29 female; median-age 55 years), which were surgically diagnosed, underwent preoperative dynamic contrast-enhanced CT. PNETs were classified based on contrast enhancement patterns in the pancreatic phase: iso/hypo-PNETs were defined as tumors containing areas of iso- or hypoattenuation except for cystic components, and hyper-PNETs were tumors showing hyperattenuation over the whole area. CT findings and contrast-enhancement patterns of the tumors were evaluated retrospectively by two radiologists and compared with the pathological grading.

Results: Iso/hypo-PNETs comprised 26 tumors, and hyper-PNETs comprised 35 tumors. Not only hyper-PNETs but also most iso/hypo-PNETs showed peak enhancement in the pancreatic phase and a washout from the portal venous phase to the delayed phase. Iso/hypo-PNETs showed larger tumor size than the hyper-PNETs (mean, 3.7 cm vs. 1.6 cm; $P < 0.001$), and were significantly correlated with unclear tumor margins ($n = 4$ vs. $n = 0$; $P = 0.029$), the existence of cystic components ($n = 10$ vs. $n = 3$; $P = 0.006$), intratumoral blood vessels in the early arterial phase ($n = 13$ vs. $n = 3$; $P < 0.001$), and a smooth rim enhancement in the delayed phase ($n = 12$ vs. $n = 6$; $P = 0.019$). Iso/hypo-PNETs also showed significantly higher pathological grading (WHO 2010 classification; iso/hypo, G1 = 14, G2 = 11, G3 = 1; hyper, G1 = 34, G2 = 1; $P < 0.001$).

Conclusion: PNETs containing iso/hypo-areas showed a rapid enhancement pattern as well as hyper-PNETs, various radiological features and higher malignant potential.

1. Introduction

Pancreatic neuroendocrine tumors (PNETs) are rare pancreatic tumors that originate from pluripotent stem cells in the ductal epithelium of the pancreas [1]. PNETs account for fewer than 3% of all pancreatic neoplasm and principally affect people in the fifth to seventh decades with no gender predilection [1–4]. Most cases are sporadic; however, some are associated with familial syndromes such as multiple endocrine neoplasia type 1 (MEN1), von Hippel-Lindau syndrome and neurofibromatosis type 1 [1,2]. Recently, the incidence of PNETs has increased, probably because of the development and widespread use of imaging modalities and improvement in the classification of PNETs [2,3,5]. In 2010, the World Health Organization (WHO) revised the grading system for PNETs [6,7]. PNETs are classified into three grades based on the mitotic count and Ki-67 index: G1, mitotic count <2 per 10 high-power fields (HPF) and/or Ki-67 ≤2%; G2, mitotic count 2–20 per 10HPF and/or Ki-67 3–20%; G3, mitotic count >20 per 10HPF and/or Ki-67 >20%.

Dynamic contrast-enhanced computed tomography (CT) is a useful modality for the detection and staging of PNETs [1,8–10]. These tumors are typically seen as well-circumscribed, hyperattenuating solid masses at the pancreatic phase images because of their hypervascular nature [1,9–15]. However, some PNETs have iso- or hypoattenuation areas compared with the normal pancreatic parenchyma in the pancreatic phase [9,10]. In that case, it may be difficult to diagnose PNETs correctly and distinguish them from pancreatic ductal adenocarcinomas, acinar cell carcinomas, or other pancreatic tumors [16]. However, there are few reports about

Abbreviations: PNETs, pancreatic neuroendocrine tumors; MEN1, multiple endocrine neoplasia type 1; WHO, the World Health Organization; HPF, high-power fields; CT, computed tomography; HU, Hounsfield units; ROI, region of interest.

* Corresponding author. Fax: +81 52 744 2335.
E-mail addresses: ryouta771@med.naogoya-u.ac.jp (R. Hyodo), Kojiro@med.naogoya-u.ac.jp (K. Suzuki), ogawa.hiroshi@h.mbox.nagoya-u.ac.jp (H. Ogawa), tidai@med.nagoya-u.ac.jp (T. Komada), naganawa@med.nagoya-u.ac.jp (S. Naganawa).

http://dx.doi.org/10.1016/j.ejrad.2015.08.014
0720-048X/

the characteristics of PNETs containing areas of iso- or hypoattenuation. The purpose of this study is to determine the characteristics of PNETs containing areas of iso- or hypoattenuation in the pancreatic phase on dynamic contrast-enhanced CT images, and the relationship with the pathological grading.

2. Materials and methods

2.1. Patients

Our institutional review board approved the retrospective collection of data and analysis for this study, and the need for informed consent from the patients was waived. CT examinations were performed in accordance with the established clinical standards of our institution, and each patient agreed to undergo examination after the purpose, methods, and risks were fully explained.

Our institution holds a prospectively maintained database of patients referred for CT examinations for detailed evaluation of known or suspected diseases of the pancreas. From this database, consecutive patients with PNET between June 2006 and March 2014, which were surgically diagnosed, were selected retrospectively. Then, we identified 80 PNETs in 59 patients. Exclusion criteria were as follows: tumor size less than 5 mm in diameter (18 tumors) and undetectable on CT even retrospectively (1 tumor).

Finally, 61 PNETs in 58 consecutive patients (29 males, 29 females; age range 18–78 years; median age 55 years) were examined in our study. Among these patients, one patient had two tumors and another patient had three tumors; the other 56 patients had a single tumor each. Clinical findings, such as a patient age, sex, the presence of MEN1 syndrome and other hereditary syndromes, were extracted from medical records. Simultaneous lymph node metastasis was determined from the pathological report or the CT follow-up. If a lymph node showed a minimal diameter of 10 mm or more at the first CT examination and became larger 6 months after, we diagnosed the lymph node as having a metastasis. Simultaneous liver metastasis was determined from the pathological report or the surgical report. Pathological grading was made in accordance with the WHO 2010 guidelines.

2.2. Dynamic CT protocol

At our institution, CT examination was performed using a 64-channel multisection CT system (Aquilion, Toshiba Medical System, Tokyo, Japan) before January 2014 ($n = 57$) and a 320-channel multisection CT system (Aquilion ONE, Toshiba Medical System, Tokyo, Japan) after that time ($n = 1$). Non-ionic contrast material (2.0–2.5 mL/kg) with an iodine concentration of 300 mg/mL was injected through a peripheral venous line within 30 s (with an upper limit of 5 mL/s), and a saline flush was injected at a fixed rate of 5 mL/s within 5 s immediately after contrast material injection. After unenhanced images had been acquired, all patients underwent early arterial, pancreatic, portal venous and delayed phase imaging. Individualized scan delays were determined using the automatic bolus-tracking method (SureStart, Toshiba Medical Systems). Average scan delays from injection of contrast material to the start of the early arterial, pancreatic, portal venous and delayed phase imaging for the 64-channel and 320-channel multisection CTs were 26, 44, 75, and 210 s, respectively. CT image analysis was performed using unenhanced images with a 5-mm section thickness at 5-mm intervals and axial enhanced images with a 2-mm section thickness at 2-mm intervals.

2.3. CT image analysis

The interval between CT imaging and surgical resection of the tumor in all 58 patients was 2–86 days (mean 33 days). The delayed phases of four tumors in 4 patients were not acquired; therefore, we evaluated 57 tumors in the delayed phase.

All CT images were assessed retrospectively by consensus between two radiologists, both with 11 years of experience in abdominal imaging, who were only aware that the patients were diagnosed with PNET histopathologically.

Visual inspection and CT values [Hounsfield units (HU)] of the tumors were evaluated on unenhanced images and for each dynamic phase. The visual inspection included two attenuation types, namely, hyperattenuation, and iso- or hypoattenuation compared with normal pancreatic parenchyma. If the tumor contained both attenuation types, we defined the largest attenuation area as the 1st domain and the 2nd largest area as the 2nd domain, and evaluated these respectively. To evaluate the CT value, a round region of interest (ROI) was drawn over the areas of the 1st and 2nd domains. The ROI size was at least 20 mm^2. Care was taken to avoid regions of tumor calcification, cystic component, and adjacent vasculatures. The ROI was drawn in the same position of the tumor at the unenhanced images and each dynamic phase. In addition, the CT value of downstream normal pancreatic parenchyma was measured.

All tumors were also evaluated for the following features: (a) maximum tumor diameter; (b) tumor location: head, neck, body, or tail of the pancreas; (c) tumor shape: round, oval, or lobulated; (d) tumor margin: well-circumscribed or poorly circumscribed; (e) cystic components (Fig. 1a); (f) calcification (Fig. 1b); (g) identification of intratumoral blood vessels in the early arterial phase (Fig. 1c); (h) smooth rim enhancement in the delayed phase: thin, wall-like rim enhancement of the tumor in the delayed phase (Fig. 1d); (i) dilatation of the main pancreatic duct: defined as a diameter of the main pancreatic duct equal to or exceeding 4 mm; (j) upstream pancreatic atrophy: defined as atrophy of pancreatic parenchyma on the upstream side of the tumor compared with the downstream side; (k) dilatation of the common bile duct: defined as a diameter of the common bile duct equal to or exceeding 10 mm; (l) vascular invasion: invasion of the common hepatic artery, splenic artery and vein, gastroduodenal artery, superior mesenteric artery and vein, and portal vein was evaluated. The criteria were vessel occlusion, stenosis or more than half of the perimeter being in contact with the tumor.

These data were collected and analyzed by another radiologist with 4 years' experience in the interpretation of abdominal images. Tumors were categorized into four types according to their attenuation patterns in the pancreatic phase: (a) PNETs showing hyperattenuation of the whole area [type 1] (Fig. 2a); (b) PNETs showing hyperattenuation of the 1st domain and iso- or hypoattenuation of the 2nd domain [type 2] (Fig. 2b); (c) PNETs showing iso- or hypoattenuation of the 1st domain and hyperattenuation of the 2nd domain [type 3] (Fig. 2c); or (d) PNETs showing iso- or hypoattenuation of the whole area [type 4] (Fig. 2d). We evaluated the radiological, pathological and clinical features of PNETs containing areas of iso- or hypoattenuation (types 2–4; iso/hypo-PNETs), and we compared iso/hypo-PNETs with PNETs showing hyperattenuation of the whole area (type 1; hyper-PNETs).

We also evaluated the correlation between the peak enhancement phase of the tumor and the pathological grading. As for the iso/hypo-PNETs, we evaluated iso/hypo-areas: the 2nd domain of type 2 tumors, the 1st domain of type 3 tumors and type 4 tumors.

In addition, we evaluated the correlation between the pathological grading and dynamic contrast enhancement patterns (pancreatic phase and delayed phase) categorized into four enhancement patterns: (a) hyper–hyper PNETs; hyper-PNETs showing hyperattenuation of the whole area compared with normal pancreatic parenchyma in the delayed phase, (b) hyper-iso/hypo PNETs; hyper-PNETs containing iso/hypo-areas in the delayed phase, (c) iso/hypo-hyper PNETs; iso/hypo-PNETs show-

Please cite this article in press as: R. Hyodo, et al., Pancreatic neuroendocrine tumors containing areas of iso- or hypoattenuation in dynamic contrast-enhanced computed tomography: Spectrum of imaging findings and pathological grading, Eur J Radiol (2015), http://dx.doi.org/10.1016/j.ejrad.2015.08.014

Fig. 1. Imaging findings of pancreatic neuroendocrine tumors (PNETs). (a) A 68-year-old man with PNET showing cystic components: a pancreatic phase image shows a round mass (arrow) in the pancreatic head with non-contrasting areas inside the tumor, which indicates cystic components. (b) A 62-year-old woman with PNET showing calcification: a delayed phase image shows a lobulated mass (arrow) in the pancreatic tail with ring-like calcification (arrowhead). (c) A 60-year-old man with PNET showing intratumoral blood vessels: an early arterial phase image shows a lobulated mass in the pancreatic tail with arteries inside the tumor (arrow). (d) A 59-year-old man with PNET showing a smooth rim enhancement: a delayed phase image shows an oval mass in the pancreatic neck with a smooth rim enhancement (arrow).

ing hyperattenuation of the whole area in the delayed phase, (d) iso/hypo-iso/hypo PNETs; iso/hypo-PNETs containing iso/hypo-areas in the delayed phase.

2.4. Statistical analysis

We used Mann–Whitney's *U* test to compare continuous variables or ordered variables, and chi-square test or Fisher's exact test was used to compare categorical variable. For statistical analysis, we used Excel® 2010 (Microsoft Corp, Redmond, WA, USA). A *P* value less than 0.05 was considered statistically significant.

3. Results

3.1. Clinical and radiological findings

The clinical and radiological findings of the 61 PNETs are summarized in Table 1. Thirty-five tumors (57%) were classified as type 1, seven (11%) as type 2, six (10%) as type 3, and 13 (21%) as type 4. There were no statistically significant differences in PNET attenuation type according to patient sex (iso/hypo-PNETs: 12 male, 14 female; hyper-PNETs: 19 male, 16 female; $P = 0.356$). Six patients (10%) were diagnosed as having MEN1 syndrome, but no other hereditary syndromes were detected. One patient with MEN 1 syndrome had two tumors, which were classified into iso/hypo-PNETs and hyper-PNETs, respectively; therefore, 5 patients had iso/hypo-PNETs and 2 patients had hyper-PNETs ($P = 0.110$).

Based on the WHO 2010 classification, there were 48 (79%) G1 tumors, 12 (20%) G2 tumors and one G3 tumor. Almost half of the iso/hypo-PNETs were G2 or G3 tumors (G2; 42%, $n = 11/26$ and G3; 4%, $n = 1/26$), although most hyper-PNETs (97%, $n = 34/35$) were G1 tumors. There was a statistically significant difference between the two groups ($P < 0.001$).

The tumor size was significantly larger for iso/hypo-PNETs (mean ± standard deviation, 3.7 ± 2.5 cm) than for hyper-PNETs (1.6 ± 0.9 cm) ($P < 0.001$). For the tumor margin, there was a statistically significant difference between the two groups ($P = 0.029$). However, most iso/hypo-PNETs (85%, $n = 22/26$) and all

Please cite this article in press as: R. Hyodo, et al., Pancreatic neuroendocrine tumors containing areas of iso- or hypoattenuation in dynamic contrast-enhanced computed tomography: Spectrum of imaging findings and pathological grading, Eur J Radiol (2015), http://dx.doi.org/10.1016/j.ejrad.2015.08.014

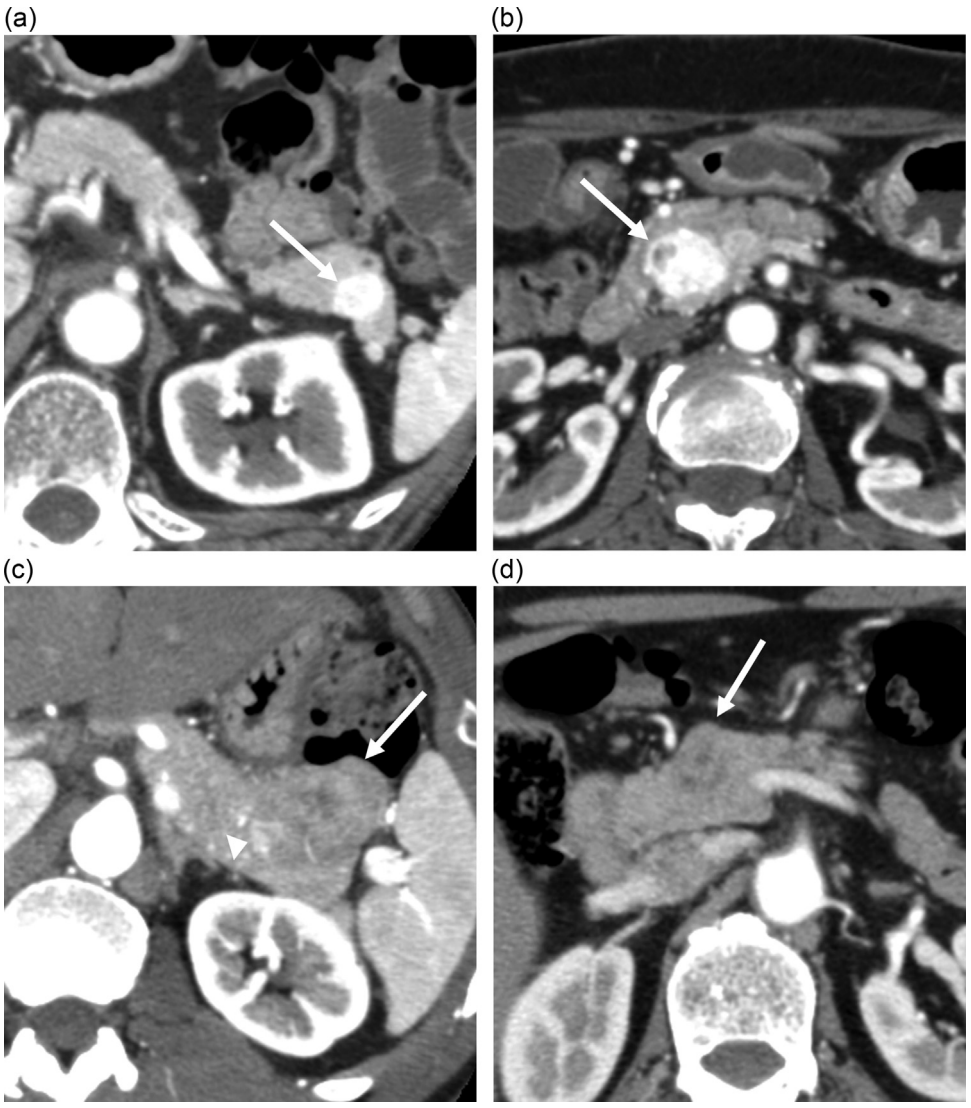

Fig. 2. Classification of tumor enhancement types. (a–d) Pancreatic phase. (a) A 68-year-old man with type 1 PNET: the tumor shows a hyperattenuation over the whole area (arrow) compared with a normal pancreatic parenchyma. (b) A 70-year-old woman with type 2 PNET: the tumor shows a hyperattenuation as a 1st domain, but contains a small area of iso- and hypoattenuation as a 2nd domain (arrow). This iso- and hypoattenuation area shows a strong enhancement in the delayed phase. (c) A 53-year-old man with type 3 PNET: the tumor shows hypoattenuation as a 1st domain (arrow), but contains a small area of hyperattenuation as a 2nd domain (arrowhead). (d) A 59-year-old man with type 4 PNET: the tumor shows an iso- or hypoattenuation at the whole area (arrow). No hyperattenuation area is detected. This is the same tumor as Fig. 1d.

hyper-PNETs (100%, $n = 35/35$) demonstrated well-circumscribed margins. In terms of tumor location and shape, there was no statistically significant difference between the two groups.

Cystic components and intratumoral blood vessels in the early arterial phase were significantly more frequent in iso/hypo-PNETs than hyper-PNETs ($P = 0.006$ and $P < 0.001$). A smooth rim enhancement in the delayed phase was detected in 18 of 57 tumors (32%), and this finding was significantly more frequent in iso/hypo-PNETs than hyper-PNETs (48% vs. 19%; $P = 0.019$). In addition, 8 of 12 (67%) G2 tumors showed this finding. Lymph node metastasis was only detected in iso/hypo-PNETs (pathological report, $n = 5$; CT follow-up, $n = 0$), and there was a statistically significant difference ($P = 0.011$). However, calcification, main pancreatic duct dilatation, upstream pancreatic atrophy, common bile duct dilatation, and liver metastasis had no significant difference between the two groups. Vascular invasion was only seen in two cases; one of the superior mesenteric vein in type 2 and the other of the splenic vein in type 4. Both tumors showed intermediate malignancy (G2) and were comprised of iso/hypo-PNETs.

3.2. CT values and peak enhancement phase of the tumors

The correlation between the peak enhancement phase and pathological grading is showed in Table 2. All hyper-PNETs showed peak enhancement up to the pancreatic phase (early arterial phase, $n = 1$; pancreatic phase, $n = 34$). On the other hand, 73% ($n = 19/26$) of iso/hypo-PNETs, and especially 69% ($n = 9/13$) of type 4 tumors, showed peak enhancement in the pancreatic phase. These tumors showed a washout pattern from the portal venous phase to the delayed phase. Similarly, normal pancreatic parenchyma showed peak enhancement in the pancreatic phase and a washout from the portal venous phase to the delayed phase.

In total, 12% ($n = 3/26$) of iso/hypo-PNETs showed peak enhancement in the portal venous phase, and 15% ($n = 4/26$) of iso/hypo-PNETs showed in the delayed phase, whereas no hyper-PNETs showed in both phases. Eighty-six percent ($n = 6/7$) of tumors that showed peak enhancement in the portal venous or delayed phase were G1 tumors, and there was no relationship between peak enhancement phase and pathological grading.

Please cite this article in press as: R. Hyodo, et al., Pancreatic neuroendocrine tumors containing areas of iso- or hypoattenuation in dynamic contrast-enhanced computed tomography: Spectrum of imaging findings and pathological grading, Eur J Radiol (2015), http://dx.doi.org/10.1016/j.ejrad.2015.08.014

Table 1
Clinical and radiological features of 61 pancreatic neuroendocrine tumors (PNETs) in 58 patients.

	Iso- or hypoattenuation PNETs		Hyperattenuation PNETs	*P* value[b]
	Total	[Types 2–4]	Type 1	
Number	26	[7,6,13]	35	
WHO classification				<0.001
G1	14 (54)	[3,3,8]	34 (97)	
G2	11 (42)	[4,3,4]	1 (3)	
G3	1 (4)	[0,0,1]	0 (0)	
Tumor diameter				<0.001
<2 cm	7 (27)	[1,1,5]	28 (80)	
>2 cm	19 (73)	[6,5,8]	7 (20)	
Location				0.079
Head	7 (27)	[3,1,3]	13 (37)	
Neck	4 (15)	[1,1,2]	6 (17)	
Body	3 (12)	[0,0,3]	10 (29)	
Tail	12 (46)	[3,4,5]	6 (17)	
Shape				0.060
Round	8 (31)	[1,1,6]	21 (60)	
Oval	8 (31)	[2,2,4]	8 (23)	
Lobulated	10 (38)	[4,3,3]	6 (17)	
Margin				0.029
Well circumscribed	22 (85)	[6,5,11]	35 (100)	
Poorly circumscribed	4 (15)	[1,1,2]	0 (0)	
Cystic component	10 (38)	[2,3,5]	3 (9)	0.006
Calcification	2 (8)	[1,0,1]	3 (9)	0.641
Intratumoral blood vessels	13 (50)	[5,3,5]	3 (9)	<0.001
Smooth rim enhancement in the delayed phase[a]	12 (48)	[2,3,7]	6 (19)	0.019
Main pancreatic duct dilatation	5 (19)	[1,1,3]	4 (11)	0.311
Upstream pancreatic atrophy	5 (19)	[1,1,3]	3 (9)	0.201
Common bile duct dilatation	3 (12)	[2,0,1]	0 (0)	0.072
Lymph node metastasis	5 (19)	[3,0,2]	0 (0)	0.011
Liver metastasis	2 (8)	[0,0,2]	1 (3)	0.388

Note: Unless otherwise specified, data are numbers of tumors, with percentage in parentheses.
[a] Total 57 tumors that underwent delayed phase imaging; Hyper-PNETs, $n = 32$; Iso/hypo-PNETs, $n = 25$.
[b] Mann–Whitney's *U* test, Chi-square test or Fisher's exact test were used for analyses.

Table 2
Correlation between peak enhancement phase and pathological grading.

	Iso- or hypoattenuation PNETs				Hyperattenuation PNETs			
	G1	G2	G3	Total	G1	G2	G3	Total
Early arterial phase	0	0	0	0	1	0	0	1
Pancreatic phase	8	10	1	19	33	1	0	34
Portal venous phase	2	1	0	3	0	0	0	0
Delayed phase	4	0	0	4	0	0	0	0

PNET, pancreatic neuroendocrine tumor.

3.3. Correlation between the dynamic contrast enhancement patterns and pathological grading

The comparison between the dynamic contrast-enhancement CT patterns and the pathological grading was follows: hyper–hyper PNETs, G1 = 21, G2 = 0; hyper-iso/hypo PNETs, G1 = 10, G2 = 1; iso/hypo-hyper PNETs, G1 = 4, G2 = 4; and iso/hypo-iso/hypo PNETs, G1 = 9, G2 = 7, G3 = 1.

4. Discussion

PNETs are typically seen as hypervascular tumors in the pancreatic phase of dynamic contrast-enhanced CT, but occasionally they contain iso- or hypoattenuated areas. In previous studies, it was reported that high-grade PNETs showed lower enhancement than low-grade PNETs [17,18]. However, few reports showed the characteristics of iso/hypo-PNETs with regard to their clinical, morphological and pathological features. In this study, we examined the characteristics of iso/hypo-PNETs using multi-phase dynamic CT, and compared them with the hyper-PNETs.

In the present study, 43% of PNETs contained iso/hypo-areas, and in particular 21% of PNETs showed iso- or hypoattenuation over their whole area. Worhunsky et al. [14] reported that 32% of PNETs contained iso/hypo-areas and 20% of PNETs showed isoenhancing or homogeneously hypoenhancing. Rodallec et al. [19] also reported that 39% of PNETs showed iso- or hypoattenuation compared with normal pancreatic parenchyma in the pancreatic phase. Therefore, our results were similar to previous reports. In addition, our results suggested that PNETs with poorly contrasting areas are not rare, and closer attention is necessary for diagnosis.

Interestingly, most iso/hypo-areas showed peak enhancement in the pancreatic phase and demonstrated a washout over time, as well as hyper-PNETs. This result indicated that most PNETs were naturally hypervascular tumors, even if iso- or hypoattenuation areas compared with the normal pancreatic parenchyma were pointed out visually. This may be because the visual contrast enhancement pattern of the tumor was decided by comparison with the contrast enhancement pattern of normal pancreatic parenchyma, which showed a rapid-washout pattern on dynamic contrast-enhanced CT. We also found that the intratumoral blood vessels in the early arterial phase were pointed out in 50% of

Please cite this article in press as: R. Hyodo, et al., Pancreatic neuroendocrine tumors containing areas of iso- or hypoattenuation in dynamic contrast-enhanced computed tomography: Spectrum of imaging findings and pathological grading, Eur J Radiol (2015), http://dx.doi.org/10.1016/j.ejrad.2015.08.014

iso/hypo-PNETs, and this finding supports the idea that most iso/hypo-PNETs are hypervascular tumors. These findings were also found in type 4 tumors, which may help to distinguish type 4 tumors from pancreatic ductal adenocarcinomas with persistent or delayed enhancement patterns. On the other hand, 15% of iso/hypo-PNETs showed peak enhancement in the delayed phase. Histopathological studies reported that some PNETs had abundant fibrous tissue [20,21]. Thus, PNETs showing delayed enhancement may have abundant fibrous tissue, although we did not compare with the pathological findings.

Our study showed that iso/hypo-PNETs were significantly correlated with higher pathological grading. d'Assignies et al. [22] described that lower blood flow in perfusion CT correlated with PNETs with higher Ki-67 proliferation index. Rodallec et al. [19] showed lower vessel density, as determined by light microscopy, was correlated with poorer differentiation of tumors and lower contrast enhancement. From these reports and our result, it may be indicated that iso/hypo-PNETs have lower vascularity and higher malignancy than hyper-PNETs.

Iso/hypo-PNETs were larger in size than hyper-PNETs, and this also matched previous reports [18,22,23]. In addition, iso/hypo-PNETs show various radiological features, such as unclear tumor margins, cystic components, intratumoral blood vessels in the early arterial phase, and smooth rim enhancement in the delayed phase. Of these findings, the unclear tumor margin and the existence of intratumoral blood vessels in the early arterial phase were possibly caused by iso- or hypoattenuation compared with normal pancreatic parenchyma.

In the present study, smooth rim enhancement in the delayed phase was detected in 48% (n = 12/25) of iso/hypo-PNETs and in 32% (n = 18/57) of all PNETs. The cause is uncertain because no pathological comparison was carried out. However, in general, PNETs have a fibrous capsule histopathologically [21], and there is a possibility of this being seen as the fibrous capsule of the tumor. Pancreatic ductal adenocarcinomas sometimes show a ring-like enhancement in the delayed phase, but this finding usually indicates a thick heterogeneous peripheral enhancement, which reflects a tumor having abundant fibrous tissue and a central necrotic component [24–26]. Therefore, the finding of a smooth rim enhancement in the delayed phase may be useful for the differentiation of iso/hypo-PNETs from pancreatic ductal adenocarcinomas. In addition, this finding was pointed out in 67% (n = 8/12) of G2 tumors; therefore, it might be useful for predicting malignancy. To the best of our knowledge, there are no previous reports about this finding in PNETs; therefore, further studies, including pathological examinations, are needed to confirm our observation.

As for the dynamic contrast enhancement patterns, there were no significant differences between hyper–hyper PNETs and hyper-iso/hypo PNETs in pathological grading. In addition, there were no significant differences between iso/hypo-hyper PNETs and iso/hypo-iso/hypo PNETs. Therefore, for the dynamic contrast-enhancement patterns, adding the delayed phase to the pancreatic phase was not especially useful for the evaluation of pathological grading in the present study. Furthermore, the peak enhancement phase was not correlated with the pathological grading. It was reported that PNETs with abundant fibrous stroma were correlated with higher malignancy [12,23]. Cappelli et al. [20] demonstrated that PNETs with persistent or delayed enhancement patterns had fibrous tissue histopathologically and showed higher malignancy. Therefore, there is a discrepancy between their report and our result. However, the definition of iso/hypo-PNETs was different, and our study included tumors with areas of hyperattenuation in part. On the other hand, the fact that 97% of hyper-PNETs in the present study were G1 tumors is probably the cause of the lack of a significant difference between hyper–hyper PNETs and hyper-iso/hypo PNETs.

The present study has several limitations. First, our study was retrospective and the observers were aware of the diagnosis of PNET. Second, we could not obtain interobserver variability scores for the qualitative analysis because of the consensus review by two radiologists. Third, the present study had potential selection bias. We only included cases that received total resection. Therefore, we had only one G3 tumor and few patients with metastasis. Fourth, the mean interval between CT and surgical resection was 33 days, and the disease could have progressed during that interval.

5. Conclusion

Most PNETs containing iso/hypo-areas in the pancreatic phase showed a rapid enhancement pattern as well as hyper-PNETs and normal pancreatic parenchyma. In addition, iso/hypo-PNETs had higher malignancy potential and showed various radiological features, such as the poorly circumscribed large masses, cystic components, intratumoral blood vessels in the early arterial phase, and smooth rim enhancement in the delayed phase.

Conflict of interest

The authors have no conflict of interest to declare.

References

[1] R.B. Lewis, G.E. Lattin Jr., E. Paal, Pancreatic endocrine tumors: radiologic-clinicopathologic correlation, Radiographics 30 (2010) 1445–1464.
[2] M. Fraenkel, M.K. Kim, A. Faggiano, G.D. Valk, Epidemiology of gastroenteropancreatic neuroendocrine tumours, Best Pract. Res. Clin. Gastroenterol. 26 (2012) 691–703.
[3] J.C. Yao, M. Hassan, A. Phan, C. Dagohoy, C. Leary, J.E. Mares, et al., One hundred years after carcinoid: epidemiology of and prognostic factors for neuroendocrine tumors in 35,825 cases in the United States, J. Clin. Oncol. 26 (2008) 3063–3072.
[4] A. Gallotti, R.P. Johnston, P.A. Bonaffini, T. Ingkakul, V. Deshpande, C. Fernandez-del Castillo, et al., Incidental neuroendocrine tumors of the pancreas: MDCT findings and features of malignancy, AJR Am. J. Roentgenol. 200 (2013) 355–362.
[5] E.J. Kuo, R.R. Salem, Population-level analysis of pancreatic neuroendocrine tumors 2 cm or less in size, Ann. Surg. Oncol. 20 (2013) 2815–2821.
[6] F.T. Bosman, F. Carneiro, R.H. Hruban, N.D. Theise, WHO Classification of Tumours of the Digestive System, 4th ed., International Agency for Research on Cancer, Lyon, 2010.
[7] D.S. Klimstra, I.R. Modlin, D. Coppola, R.V. Lloyd, S. Suster, The pathologic classification of neuroendocrine tumors: a review of nomenclature, grading, and staging systems, Pancreas 39 (2010) 707–712.
[8] G. Foti, L. Boninsegna, M. Falconi, R.P. Mucelli, Preoperative assessment of nonfunctioning pancreatic endocrine tumours: role of MDCT and MRI, Radiol. Med. 118 (2013) 1082–1101.
[9] A.D. Baur, M. Pavel, V. Prasad, T. Denecke, Diagnostic imaging of pancreatic neuroendocrine neoplasms (pNEN): tumor detection, staging, prognosis, and response to treatment, Acta Radiol. (2015) [Epub ahead of print].
[10] N. Kartalis, R.M. Mucelli, A. Sundin, Recent developments in imaging of pancreatic neuroendocrine tumors, Ann. Gastroenterol. 28 (2015) 193–202.
[11] J.L. Fidler, J.G. Fletcher, C.C. Reading, J.C. Andrews, G.B. Thompson, C.S. Grant, et al., Preoperative detection of pancreatic insulinomas on multiphasic helical CT, AJR Am. J. Roentgenol. 181 (2003) 775–780.
[12] R. Graziani, A. Brandalise, M. Bellotti, R. Manfredi, A. Contro, M. Falconi, et al., Imaging of neuroendocrine gastroenteropancreatic tumours, Radiol. Med. 115 (2010) 1047–1064.
[13] D. Hayashi, J.N. Tkacz, S. Hammond, B.C. Devenney-Cakir, S. Zaim, N. Bouzegaou, et al., Gastroenteropancreatic neuroendocrine tumors: multimodality imaging features with pathological correlation, Jpn. J. Radiol. 29 (2011) 85–91.
[14] D.J. Worhunsky, G.W. Krampitz, P.D. Poullos, B.C. Visser, P.L. Kunz, G.A. Fisher, et al., Pancreatic neuroendocrine tumours: hypoenhancement on arterial phase computed tomography predicts biological aggressiveness, HPB (Oxford) 16 (2014) 304–311.
[15] A. Sundin, Radiological and nuclear medicine imaging of gastroenteropancreatic neuroendocrine tumours, Best Pract. Res. Clin. Gastroenterol. 26 (2012) 803–818.
[16] S.P. Raman, R.H. Hruban, J.L. Cameron, C.L. Wolfgang, E.K. Fishman, Pancreatic imaging mimics: part 2, pancreatic neuroendocrine tumors and their mimics, AJR Am. J. Roentgenol. 199 (2012) 309–318.
[17] D.W. Kim, H.J. Kim, K.W. Kim, J.H. Byun, K.B. Song, J.H. Kim, et al., Neuroendocrine neoplasms of the pancreas at dynamic enhanced CT:

Please cite this article in press as: R. Hyodo, et al., Pancreatic neuroendocrine tumors containing areas of iso- or hypoattenuation in dynamic contrast-enhanced computed tomography: Spectrum of imaging findings and pathological grading, Eur J Radiol (2015), http://dx.doi.org/10.1016/j.ejrad.2015.08.014

comparison between grade 3 neuroendocrine carcinoma and grade 1/2 neuroendocrine tumour, Eur. Radiol. 25 (2015) 1375–1383.
[18] Y. Luo, Z. Dong, J. Chen, T. Chan, Y. Lin, M. Chen, et al., Pancreatic neuroendocrine tumours: correlation between MSCT features and pathological classification, Eur. Radiol. 24 (2014) 2945–2952.
[19] M. Rodallec, V. Vilgrain, A. Couvelard, P. Rufat, D. O'Toole, V. Barrau, et al., Endocrine pancreatic tumours and helical CT: contrast enhancement is correlated with microvascular density, histoprognostic factors and survival, Pancreatology 6 (2006) 77–85.
[20] C. Cappelli, U. Boggi, S. Mazzeo, R. Cervelli, D. Campani, N. Funel, et al., Contrast enhancement pattern on multidetector CT predicts malignancy in pancreatic endocrine tumours, Eur. Radiol. 25 (2015) 751–759.
[21] A. Kasajima, S. Yazdani, H. Sasano, Pathology diagnosis of pancreatic neuroendocrine tumors, J. Hepatobiliary Pancreat. Sci. (2015), [Epub ahead of print].
[22] G. d'Assignies, A. Couvelard, S. Bahrami, M.P. Vullierme, P. Hammel, O. Hentic, et al., Pancreatic endocrine tumors: tumor blood flow assessed with perfusion CT reflects angiogenesis and correlates with prognostic factors, Radiology 250 (2009) 407–416.
[23] S. Tatsumoto, Y. Kodama, Y. Sakurai, T. Shinohara, A. Katanuma, H. Maguchi, Pancreatic neuroendocrine neoplasm: correlation between computed tomography enhancement patterns and prognostic factors of surgical and endoscopic ultrasound-guided fine-needle aspiration biopsy specimens, Abdom. Imaging 38 (2013) 358–366.
[24] Y. Hattori, T. Gabata, Y. Zen, K. Mochizuki, H. Kitagawa, O. Matsui, Poorly enhanced areas of pancreatic adenocarcinomas on late-phase dynamic computed tomography: comparison with pathological findings, Pancreas 39 (2010) 1263–1270.
[25] Y. Sugiyama, Y. Fujinaga, M. Kadoya, K. Ueda, M. Kurozumi, H. Hamano, et al., Characteristic magnetic resonance features of focal autoimmune pancreatitis useful for differentiation from pancreatic cancer, Jpn. J. Radiol. 30 (2012) 296–309.
[26] N. Furuhashi, K. Suzuki, Y. Sakurai, M. Ikeda, Y. Kawai, S. Naganawa, Differentiation of focal-type autoimmune pancreatitis from pancreatic carcinoma: assessment by multiphase contrast-enhanced CT, Eur. Radiol. 25 (2015) 1366–1374.

Please cite this article in press as: R. Hyodo, et al., Pancreatic neuroendocrine tumors containing areas of iso- or hypoattenuation in dynamic contrast-enhanced computed tomography: Spectrum of imaging findings and pathological grading, Eur J Radiol (2015), http://dx.doi.org/10.1016/j.ejrad.2015.08.014